

# THE INDIRECT ADAPTIVE FEED-FORWARD CONTROL IN MAGNETIC BEARING SYSTEMS FOR MINIMIZING SELECTED VIBRATION PERFORMANCE MEASURES

Juan Shi

School of Communications and Informatics, Victoria University of Technology  
PO Box 14428, MCMC 8001, Victoria, Australia  
juan.shi@vu.edu.au

Ron Zmood and LiJiang Qin

School of Electrical and Computer Systems Engineering  
RMIT, Victoria 3000, Australia  
Lijiang.Qin@rmit.edu.au

## ABSTRACT

To attenuate synchronous disturbances in magnetic bearing systems, a number of approaches have been used, including both adaptive feed-forward and feedback approaches. In practice it is generally preferred to use feed-forward techniques as they have less effect on system stability. One method of feed-forward disturbance attenuation that has been proposed is the application of adaptive filtering techniques to minimize the magnitude of the magnetic bearing system error signal. This will be referred to as an "indirect" method for synchronous disturbance attenuation.

In this paper we examine two cases by using the "indirect" method of synchronous disturbance attenuation. In the first case the rotor displacement is minimized while in the second the bearing actuator current is minimized. As it is often desired to minimize displacement vibration at low speeds and minimize control effort (i.e. actuator current) at high speeds this paper also examines algorithms for smoothly transitioning from displacement vibration minimization at low speeds to current minimization at high speeds.

The paper discusses both the simulation of these algorithms and their experimental testing on the RMIT magnetic bearing test stand.

## 1 INTRODUCTION

It is well known that active magnetic bearings (AMBs) have many unique features including low friction wears, efficient operation at high speed, and

elimination of lubricants, etc. Hence AMBs are used in a number of applications such as energy storage flywheels, high-speed turbines and compressors [1].

AMB actuators are open-loop unstable, and, therefore, feedback control is essential for achieving stabilization and good performance. Shafts (rotors) in AMB systems are supposed to be rotating at high speed. As they unavoidably have unbalanced masses, disturbance forces are generated when the shafts are rotating. These disturbance forces, being referred to as synchronous disturbances, are most significant at high frequencies because their amplitudes increase with the square of the shaft rotating speed. Due to the synchronous disturbances, the rotors may move away from the centre of the bore of the AMB actuators, and may possibly collide with the touching-down bearings.

To attenuate synchronous disturbances in AMB systems, two approaches have been used. In the first approach [2] the objective is to keep the shaft rotate around its geometric centre in the presence of synchronous disturbances, and is to be referred to as *displacement nulling*. To this end, electro-magnetic forces at the synchronous frequency need to be generated in the AMB systems so as the effective stiffness of the bearing system to unbalanced forces are increased.

In the second approach a control system is designed such that it allows the shaft to rotate around its axis of inertia, and is referred to as automatic balancing in the literature [3] as no unbalance force is acting on the shaft in this case. As the required currents in bearing actuators are small in this approach,

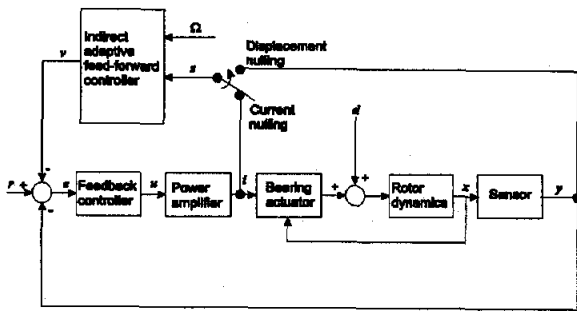


Figure 1: Indirect adaptive feed-forward control for attenuating synchronous disturbances in magnetic bearing systems

it is also referred to as *current nulling* approach.

This paper further investigates an adaptive feed-forward approach for adjusting the amplitude and phase of the synchronous signal so as to achieve displacement and current nulling. In implementing the adaptive feed-forward displacement (current) nulling controller, the *displacement (current)* signal is used as the main input signal of the controller. However, in the adaptation algorithm the *error signal* between the input *displacement (current)* signal and the generated signal from the adaptive filter is used as the vibration performance measure. Hence, this method is referred to as an "indirect" method for synchronous disturbance attenuation. In addition, the switching algorithm between displacement and current nulling is also investigated. Both simulation and experimental results show the effectiveness of the adaptive algorithm. Simulations and experiments are also carried out for testing a switching algorithm between displacement and current nulling. Methods using the *displacement (current)* signal as the main input signal of the displacement (current) nulling controller and the *displacement (current)* signal is also used as the performance measure in the adaptation algorithm is referred to as a "direct" method and is detailed in a paper in reference [9].

## 2 CONTROLLER STRUCTURE AND ALGORITHM

### 2.1 Controller Structure

Figure 1 shows the proposed controller structure for attenuating synchronous disturbances in magnetic bearing systems. A feedback control loop is used for stabilizing the system while an "indirect" adaptive feed-forward controller is employed to attenuate synchronous disturbances.

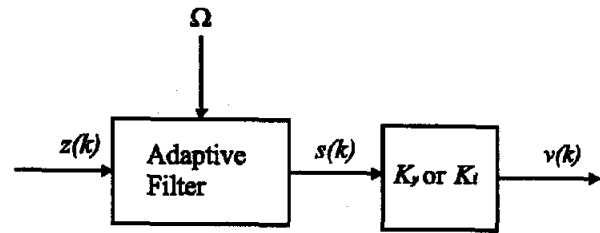


Figure 2: Structure of the "indirect" adaptive feed-forward controller for displacement or current nulling

It should be noted that in Figure 1, the shaft angular speed  $\Omega$  which can be easily measured in practice is one of the two input signals to the feed-forward adaptive controller. The second input signal  $z$  can be chosen to be either the current  $i$  or displacement  $y$  depending upon whether current nulling or displacement nulling is desired.

It is also noted that Betschon et. al. and Zhao et. al. [4][5] used *displacement signal*  $y$  as the input signal to the adaptive feed-forward controller, and the performance measure used was the mean square of the difference between signal  $y$  and  $v$ . The control effect is equivalent to the *current nulling* approach in this paper. In this paper, the displacement nulling and current nulling are further investigated and it is found that a gain  $K_y$  or  $K_i$  needed to be introduced so that displacement nulling can be achieved with the displacement  $y$  as the input signal and current nulling can be achieved with the current  $i$  as the input signal to the adaptive feed-forward controller.

The structure of the proposed "indirect" adaptive feed-forward controller is further shown in Figure 2, which consists of an adaptive filter and a gain  $K_y$  or  $K_i$  for displacement or current nulling respectively. The adaptive filter is used to estimate the amplitude and phase of the synchronous disturbance, while gain  $K_y$  or  $K_i$  is used for adjusting the control signal amplitude in the direction determined by the adaptive filter.

### 2.2 Adaptive Algorithm

This section is focused on the derivation of the adaptive algorithms for displacement nulling and current nulling. A detailed discussion of displacement nulling is given, while the derivation for current nulling has been omitted because of its obvious similarities.

It is assumed that the reference signal  $r$  in Figure 1 is zero for simplicity. The gain  $K_y$  in Figure 2 is important for achieving good vibration attenuation performance and is related to the closed-loop gain from output displacement signal  $y$  to the generated input signal  $v$  as shown in Figure 1.  $K_y$  is to be

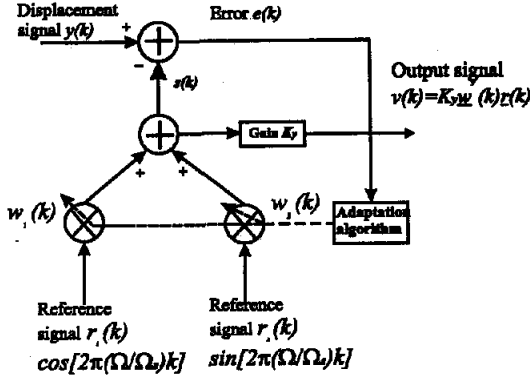


Figure 3: Structure of the "indirect" adaptive displacement nulling feed-forward controller

adjusted in implementation.

Figure 3 shows a detailed structure of the "indirect" displacement nulling feed-forward controller, where  $\Omega_s$  represents the sampling frequency in rad/s and  $T$  is the sampling period, i.e.  $\Omega_s = \frac{2\pi}{T}$ . Two reference signals  $r_1(k)$  and  $r_2(k)$  are adjusted by two weighting functions  $w_1(k)$  and  $w_2(k)$  to generate an estimation of the synchronous disturbance signal in  $y(k)$  [4],[5]. These weighting functions are to be updated using the adaptive algorithm derived below.

The vector form of the two reference signals is:

$$\underline{r}(k) = \begin{bmatrix} r_1(k) \\ r_2(k) \end{bmatrix} = \begin{bmatrix} \cos(2\pi \frac{\Omega}{\Omega_s} k) \\ \sin(2\pi \frac{\Omega}{\Omega_s} k) \end{bmatrix} \quad (1)$$

Assume that the input displacement signal to the adaptive vibration controller is:

$$y(k) = A_y \cos(2\pi \frac{\Omega}{\Omega_s} k + \Phi_y) \quad (2)$$

The generated signal from the adaptive FIR filter is:

$$s(k) = \underline{w}^T(k) \underline{r}(k) \quad (3)$$

whereas the Fourier coefficients vector

$$\underline{w}(k) = \begin{bmatrix} w_1(k) \\ w_2(k) \end{bmatrix}$$

The objective of the adaptation algorithm is to minimize the following vibration performance measure or cost function:

$$J(\underline{w}) = E\{e^2(k)\} \quad (4)$$

where  $E\{\cdot\}$  is the expectation operator and

$$e(k) = y(k) - s(k) = y(k) - \underline{w}^T(k) \underline{r}(k) \quad (5)$$

Since the performance measure used here is not directly proportional to the displacement signal but

the error signal, hence this method is referred to as the "indirect" method.

Assuming that the signals  $y(k)$  and  $\underline{r}(k)$  are weakly stationary, the mean square error (MSE) can be calculated as follows:

$$\begin{aligned} MSE = J(\underline{w}) &= E\{e^2(k)\} \\ &= E\{y^2(k)\} + \underline{w}^T(k) E\{\underline{r}(k) \underline{r}^T(k)\} \underline{w}(k) \\ &\quad - 2\underline{w}^T(k) E\{y(k) \underline{r}(k)\} \end{aligned} \quad (6)$$

Defining the auto-correlation matrix  $\mathbf{R}$  and the cross-correlation vector  $\underline{p}$  as:

$$\mathbf{R} = E\{\underline{r}(k) \underline{r}^T(k)\} \quad (7)$$

$$\underline{p} = E\{y(k) \underline{r}(k)\} \quad (8)$$

Finally the vibration performance measure or cost function can be written as

$$\begin{aligned} J(\underline{w}) &= E\{e^2(k)\} \\ &= E\{y^2(k)\} + \underline{w}^T(k) \mathbf{R} \underline{w}(k) - 2\underline{w}^T(k) \underline{p} \end{aligned} \quad (9)$$

The Least Mean Square (LMS) algorithm is used to update the weighting functions  $w_1(k)$  and  $w_2(k)$  [6][7]. The basis for the LMS algorithm is the momentary quadratic error. The momentary gradient is calculated by

$$\begin{aligned} \nabla_{\underline{w}} \{e^2(k)\} &= 2e(k) \nabla_{\underline{w}} \{y(k) - s(k)\} \\ &= 2e(k) \nabla_{\underline{w}} \{y(k) - \underline{w}^T(k) \underline{r}(k)\} \end{aligned} \quad (10)$$

The coefficient vector is updated by using the momentary gradient

$$\begin{aligned} \underline{w}(k+1) &= \underline{w}(k) - c \nabla_{\underline{w}} \{e^2(k)\} \\ &= \underline{w}(k) + 2ce(k) \underline{r}(k) = \underline{w}(k) + \mu e(k) \underline{r}(k) \end{aligned} \quad (11)$$

### 3 SWITCHING ALGORITHM BETWEEN DISPLACEMENT NULLING AND CURRENT NULLING

In displacement nulling, electro-magnetic forces at the synchronous frequency need to be generated in the AMB system so as the effective stiffness of the bearing system to unbalanced forces are increased. However, at high speed, large bearing actuator forces proportional to  $\Omega^2$  need to be generated to cancel the effect of synchronous disturbances and as these forces will be transmitted to the machine housing considerable plant vibration will occur. In that case current nulling is preferred. A fuzzy logic controller is

employed to achieve smooth transitioning from displacement vibration minimization at low speeds to current minimization at high speeds.

The fuzzy logic controller utilizes speed and peak current of the amplifier as inputs is designed to introduce a nonlinear function into the transition logic so as to prevent limit cycle operation of the adaptive feed-forward control loop and to prevent the saturation of the power amplifier. The output of the fuzzy logic controller  $\gamma$  ( $0 \leq \gamma \leq 1$ ) is adjusted according to the speed  $\Omega$  and the peak current of the power amplifier  $i_{peak}$ . If the speed  $\Omega$  is low and  $i_{peak}$  is low,  $\gamma$  is low so that the injected signal is basically for displacement nulling. If the speed  $\Omega$  is high and  $i_{peak}$  is high due to synchronous disturbances,  $\gamma$  is high so that the injected signal is basically for current nulling. If the speed  $\Omega$  is moderate and  $i_{peak}$  is not too high as to cause power amplifier saturation,  $\gamma$  is medium so that both displacement and current will be reduced at transition speeds.

## 4 SIMULATION AND EXPERIMENTAL RESULTS

The AMB system used to test the proposed adaptive feed-forward vibration control algorithms is a magnetic bearing system mounted on a test-rig in the School of Electrical and Computer Systems Engineering at RMIT University. For a detail description of the system please refer to references [8] and [9].

### 4.1 Simulation Results

Figures 4 (a) and (b) show the displacement  $x_L$  and current  $i_L$  of the magnetic bearing without the adaptive vibration controller as a function of rotor speed. Figures 4 (c) and (d) show the displacement  $x_L$  and current  $i_L$  of the magnetic bearing with the adaptive vibration controller. The shaft displacements at the left-end are denoted by  $x_L$ . The shaft currents at the left-end are denoted by  $i_L$ . For rotor speeds of 1100 rpm and above complete displacement nulling is used. From 1100 rpm to 1800 rpm, both displacement nulling and current nulling takes effects and the weighting of the two components depends on the  $\gamma$  value from the fuzzy logic controller. For the rotor speed of 1800 rpm and above complete current nulling method is employed. It can be seen from Figures 4 (c) and (d) that displacement nulling and current nulling are both very effective and the smooth transition between displacement nulling and current nulling has also been achieved.

As the performance results for the left- and right-hand bearings are similar only those for the left-hand

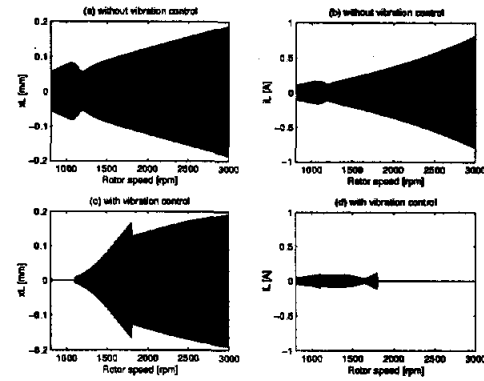


Figure 4: Displacement and current signals without nulling [(a), (b)] with complete displacement nulling (rotor speed < 1100 rpm), displacement nulling to current nulling transition (from 1100 rpm to 1800 rpm) and complete current nulling (rotor speed > 1800 rpm) [(c), (d)]

bearing is discussed in this paper.

### 4.2 Experimental Results

A digital signal processor TMS320C6701 with high speed A/D and D/A converter is used to implement the "indirect" adaptive feed-forward control algorithm. This DSP is also used for implementing the feedback control algorithm but its realization will not be examined in this paper. The shaft speed  $\Omega$  is computed by the DSP using the output pulses from the shaft toothed wheel sensor.

Figures 5 (a) and (b) show the measured displacement  $x_L$  and  $y_L$ , at the left end of the shaft, for the case where no vibration control was used and the shaft speed was fixed at 1300 rpm. To illustrate the effect of displacement nulling control the measurements were repeated with the adaptive feed-forward controller operating and the results are shown in Figures 5 (c) and (d) for the shaft again rotating at 1300 rpm. It can be readily seen that vibration amplitude has been considerably reduced.

To appreciate the effect of current nulling, Figure 6 shows the power amplifier current  $i_{xL}$  and  $i_{yL}$  measured with the shaft speed fixed at 1300 rpm. In Figures 6 (a) and (b), the currents  $i_{xL}$  and  $i_{yL}$  in the absence of current nulling are shown, while in Figures 6 (c) and (d) the case where the adaptive feed-forward controller is operating are shown. It is readily seen that there is considerable reduction in the amplitude of the coil currents in the latter case.

To further illustrate the effect of the adaptive feed-forward controllers, Figures 7 and 8 show the performance of the adaptive controller as a function of ro-

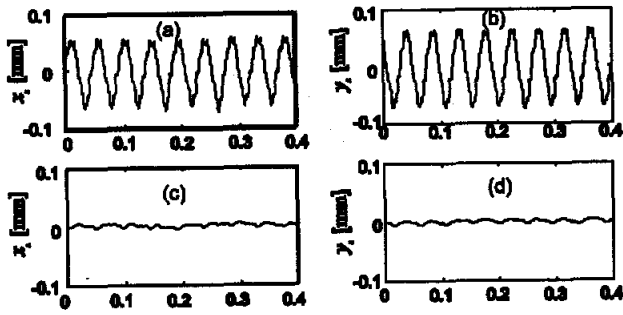


Figure 5: Shaft displacements at the left bearing without nulling [(a), (b)] and with displacement nulling [(c),(d)]

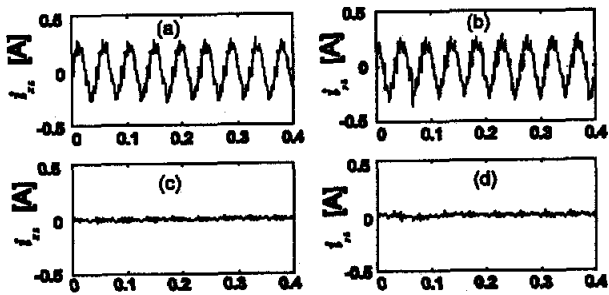


Figure 6: Power amplifier output currents for the left end bearing actuator without nulling [(a), (b)] and with current nulling control [(c),(d)]

tor speed for both displacement and current nulling. The amplitudes  $A_{xL}$ ,  $A_{yL}$ , and  $A_{ixL}$ ,  $A_{iyL}$  of the displacements  $x_L$  and  $y_L$  and currents  $i_{xL}$  and  $i_{yL}$  are shown in Figure 7 (a), (b), (c) and (d) respectively. In these figures the graphs having full lines are for the case where the adaptive controller is absent, while those with broken lines are for the case where adaptive feed-forward displacement nulling is present. It will be noted from this figure that in the absence of displacement nulling there is a distinct critical speed at about 1300 rpm. However in the case where displacement nulling controller is operating the vibration amplitude is considerably reduced and there is no evidence of any vibration resonance. The actuator current nevertheless shows a distinct peaking at 1300 rpm which indicates that considerable actuator forces are being generated to suppress the vibrations.

In Figure 8 the amplitudes  $A_{xL}$ ,  $A_{yL}$ ,  $A_{ixL}$ , and  $A_{iyL}$  are again plotted as a function of the rotor speed, for the case of adaptive feed-forward current nulling. It will be noted that the amplitudes of the actuator currents are considerably reduced compared to the case where no adaptive control is present. As a consequence the bearing forces at the synchronous

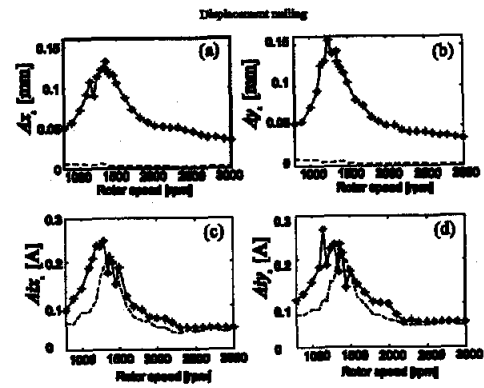


Figure 7: Bearing displacements and currents with (broken lines) and without (full lines) displacement nulling control as function of rotor speed

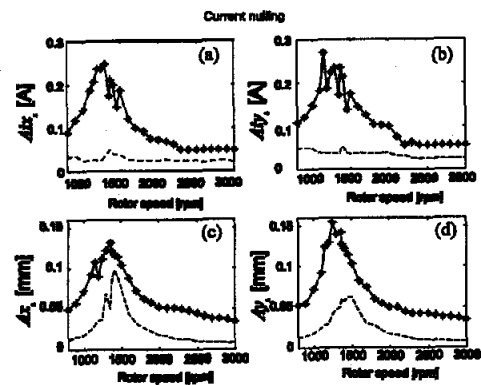


Figure 8: Bearing displacements and currents with (broken lines) and without (full lines) current nulling control as function of rotor speed

speed are negligible. It can also be seen that the displacement amplitude is increased at critical speeds compared with the case for displacement nulling as shown in Figure 7.

Figures 9 (a) and (b) show the comparison results of the vibration amplitudes of displacements and currents  $A_{xL}$ ,  $A_{yL}$ ,  $A_{ixL}$ , and  $A_{iyL}$ , without and with the adaptive feed-forward control. In the case when the adaptive feed-forward controller is operating, complete displacement nulling is employed for shaft speed below 1100 rpm and complete current nulling is employed for shaft speed above 1800 rpm. The transition occurred from 1100 to 1800 rpm in which both displacement nulling and current nulling take effects and the weighting of the two depends on the weighting function  $\gamma$ . It can be seen from this figure that the amplitudes of the displacements and currents are considerably reduced during the complete displacement and current nulling speed regions

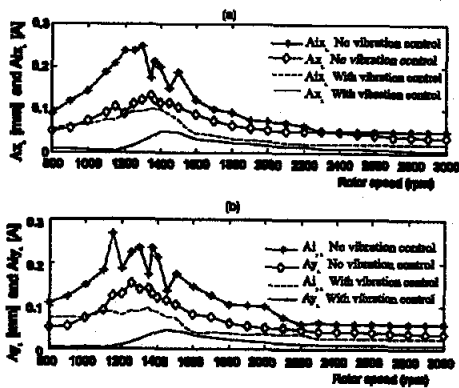


Figure 9: Bearing displacements and currents without and with complete displacement nulling, displacement to current nulling transition, and complete current nulling as a function of shaft speed

as well as during the transition period.

## 5 CONCLUSIONS

In this paper, an "indirect" adaptive feed-forward vibration control method has been proposed to achieve displacement nulling at low speeds and to achieve current nulling at high speeds. A fuzzy logic controller which utilizes speed and peak current of the power amplifier as inputs is designed to introduce smooth transition from displacement vibration minimization at low speeds to current minimization at high speeds.

The proposed "indirect" adaptive displacement and current nulling vibration control algorithms and their switching algorithm have been successfully simulated and implemented in real-time using the test rig at RMIT University, and has shown that they have considerable promise.

### ACKNOWLEDGEMENT

The first author wish to thank Victoria University of Technology for granting her six months sabbatical leave so that this research project can be carried out at RMIT. The authors also wish to thank Mr Ashraf Kadri and Mr Miroslav Miljanic for their contribution in helping to use the DSP board and in maintenance of the magnetic bearing system in the research laboratory at RMIT. This work was partially supported by an Australian Research Council SPIRT Grant.

## References

[1] H. Bleuler, C. Gahler, R. Herzog, R. Larsonneur, T. Mizuno, R. Siegart, and S. Woo, "Ap-

plication of digital signal processors for industrial magnetic bearing", *IEEE Transactions on Control Systems Technology*, Vol. 2, No. 4, pp. 280-289, December 1994.

- [2] F. Matsumura, T. Namerikawa, K.Hagiwara, and M. Fujita, "Application of Gain Scheduled Hoo Robust Controllers to a Magnetic Bearing", *IEEE Transactions on Control Systems Technology*, Vol. 4, No. 5, pp. 484-492, September. 1996.
- [3] B. Shafai, S. Beale, P. LaRocca, and E. Cusson, "Magnetic Bearing Control Systems and Adaptive Forced Balancing", *IEEE Control Systems Magazine*, Vol. 14, No. 2, pp. 4-13, April 1994.
- [4] F. Betschon and R. Schob, "On-line-adapted Vibration Control", *Proceedings of the Sixth International Symposium on Magnetic Bearings*, Massachusetts Institute of Technology, Cambridge, Massachusetts, USA, August 5-7, 1998, pp. 362- 371.
- [5] H.Zhao, L.Zhao, and W.Jiang, "Simulation and Experimental Research on Unbalance Vibration Control of AMB System", *Seventh International Symposium on Magnetic Bearings*, August 23-25, 2000, ETH Zurich, Switzerland, pp. 573-578.
- [6] C.F.N.Cowan, and P.M.Grant, "Adaptive Filters", 1985, (Prentice-Hall Inc, Englewood Cliffs, New Jersey).
- [7] B.Widrow, and S.D. Stearns, "Adaptive Signal Processing", 1985, Prentice-Hall Signal Processing Series. (Prentice-Hall Inc, Englewood Cliffs,N.J.07632).
- [8] L.J. Qin, "Micro Magnetic Bearing: Investigation on the New Design and Control Methodologies", PhD thesis, Royal Melbourne Institute of Technology, 2001.
- [9] J.Shi, R. Zmood, and L.J.Qin: "The Direct Adaptive Feed-forward Unbalance Vibration Control Methods for Magnetic Bearing Systems", to be Presented on the Seventh International Conference on Control, Automation, Robotics and Vision to be held in Singapore in December 3-6, 2002.